
Invited Talk at the International Conference on Exotic Atoms and Related Topics
September 5th - 9th, 2011 Vienna, Austria

# Collisional Processes in Exotic Atoms

Grigory KORENMAN

D.V.Scobeltsyn Institute of Nuclear Physics,
M.V. Lomonosov Moscow State University,
Moscow 119991, Russia

# CONTENTS

# 1. INTRODUCTION

Experimental discovery of long-lived $\bar{p}$ states in He (1991):
new chapter in the study of exotic atoms and of antiproton properties
▷ extended theoretical problems in the exotic-atom physics

First stage of the experimental study $\bar{p}He^+$: DATS
(Delayed Annihilation Time Spectra)
▷ general picture of the dynamic processes: formation of antiprotonic atoms, fraction of metastable states, cascade of transition *etc.*

Advanced study: Laser spectroscopy of antiprotonic helium,
Microwave spectroscopy of hyperfine structure of $\bar{p}He^+$

▷ Precision calculations of quantum 3-body system ($\bar{p}\,e\,He^{++}$) involving fine and hyperfine interactions and other subtle effects.
▷ Detailed dynamic characteristics of individual levels (primary populations, collisional quenching, shift and broadening of spectral lines *etc.*)

# 2. FORMATION of EXOTIC ATOMS

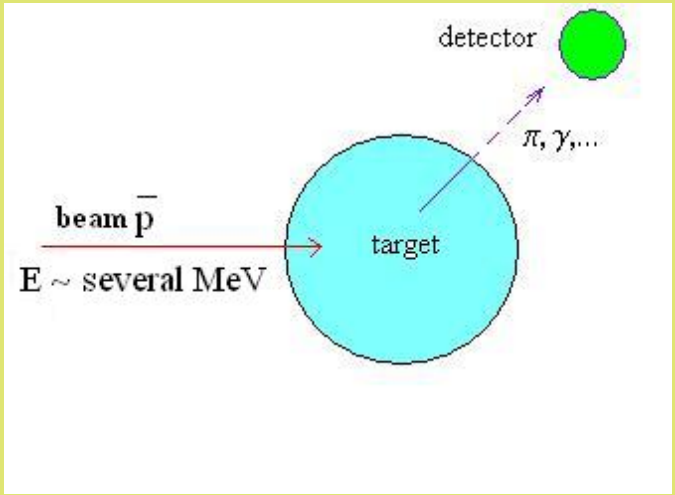


Two steps:
1) Slowing down from initial energy $E_i \sim 5$ MeV to atomic ionization potential $I_0 \sim 10 \div 20$ eV)
2) Coulomb capture into atomic orbits (in monoatomic gas target, such as He, Ne, *etc.*)
or into molecular orbits (in molecular target) followed by dissociation of the molecular complex

Competition between three types of processes in $X^- + A$ - collisions

$$X^- + A \to \begin{cases} X^- + A & \text{(elastic scattering)}, \\ X^- + A^+ + e & \text{(ionization)}, \\ (X^- A^+)^* + e & \text{(atomic capture)} \end{cases}$$

at very low kinetic energy ($\lesssim 10Z$ eV) define main features of primary characteristics of exotic-atom formation.

Long history of theoretical studies of these processes

from E.Fermi and E.Teller (1947) up to now

# Simple Model of Exotic Atom Formation in Noble Gases

"Black body" with potential "tale"

($X^-$ - He) interaction

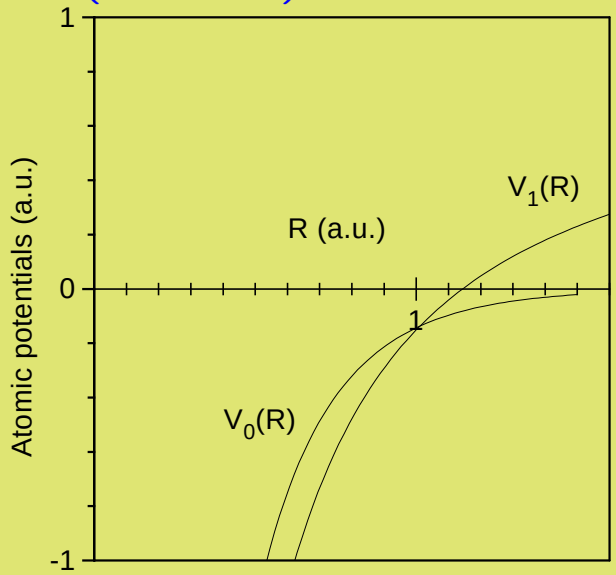


$$V_0(R): \text{ term } (X^- - A)$$

$$V_1(R): \text{ term } (X^- - A^+)$$

$$V_1(\infty) - V_0(\infty) = I_0$$

Crossing point $R_0$ is a radius of inelastic interaction.
At $R \le R_0$ electron escapes with energy

$$\epsilon_e(R) = V_0(R) - V_1(R).$$

Relative kinetic energy of $(X^- - A^+)$: $E_f = E - I_0 - \epsilon_e$.
Mean electron energy $\bar{\epsilon}_e \sim 1 \div 2$ eV. Roughly, $\epsilon \simeq 0 \Rightarrow$
$R_0$ is a "black-body" radius
$\Rightarrow$ ionization at $E > I_0$, atomic capture at $E < I_0$.

Total inelastic cross section $\sigma_r(E) = \pi\rho_0^2(E)$,
$\rho_0(E)$ is a maximum impact parameter allowing $X^-$ to reach $R_0$.

$$\rho_0^2(E) = \begin{cases} R_0^2(1 + W_0/E) & \text{if } E > E_p, \\ \sqrt{2\alpha/E} & \text{if } E > E_p \end{cases} \qquad W_0 = -V_0(R_0)$$

He: $I_0 = 0.904\,a.u. = 24.6$ eV, $R_0 \simeq 1.0\,a.u.$, $\alpha = 1.383\,a.u.$, $E_p = 0.014\,a.u.$

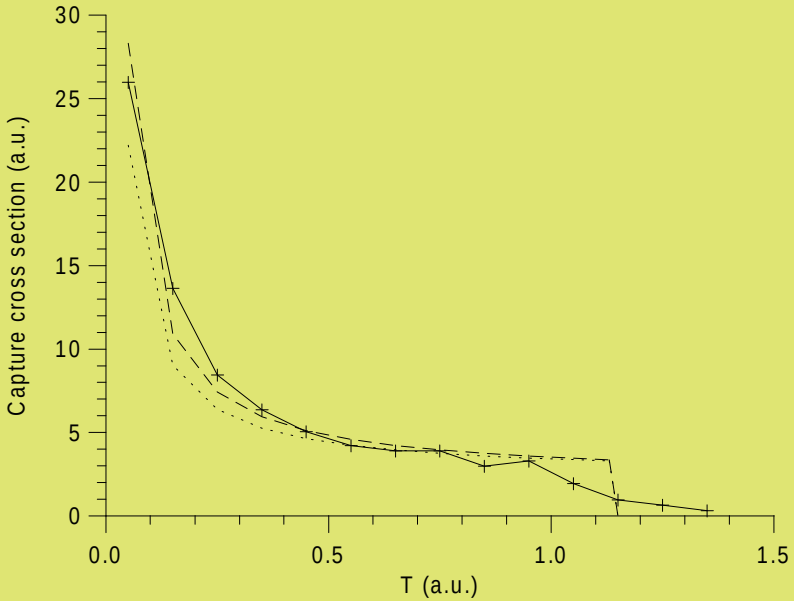


Atomic capture cross sections in $\bar{p} + He$ collisions

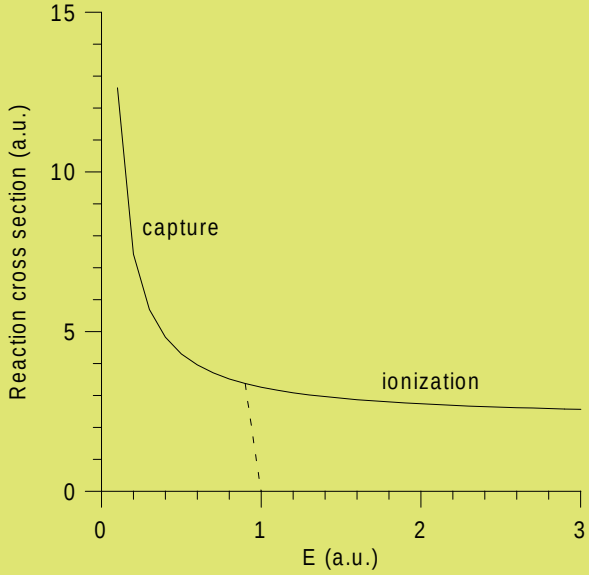


Reaction cross section in $\bar{p} + He$ collisions

## Primary Kinetic Characteristics:

Cross sections $\overset{\text{input}}{\Longrightarrow}$ Kinetic equation $\overset{\text{output}}{\Longrightarrow}$ Primary populations and distributions

### Primary distributions:

- Probability of atomic capture at c.m. kinetic energy and impact parameter:

$$w_c(E_c, b)dE_c db \simeq \theta(I_0 - E_c)\,(dE_c/I_0) \cdot \theta\,(b_m(E_c) - b)\;(db^2/b_m^2)$$

- Distribution over inner energy $E$: uniform from $E_A$ to $E_A + I_0$,

$$p(E) = (1/I_0)\theta(E - E_A)\,\theta(E_A + I_0 - E)$$

- Distribution over angular momentum $L$: cut statistical

$$p(E, L) = p(E) \cdot \theta(L_m(E) - L) \cdot (2L + 1)/[L_m(E) + 1]^2,$$

where $L_m(E) + 1/2 = \sqrt{2\mu(E + I_0)}\rho_0(E + I_0)$

- Distribution over principal quantum number:

$$p_{nL} = p(E_{nL}, L)|dE_{nL}/dn| \to\sim (1/n^3)\theta(n-n_0)\cdot(2L+1)/[L_m(n)+1]^2\cdot\theta(L_m(n)-L)$$

- Distribution over recoil kinetic energy of $(X^-A^+)^*$: uniform from 0 to $T_m = I_0 \cdot m_X/m_A$, $p(T) = \theta(T_m - T)/T_m$, $p(T; nL) = \delta(T - T_{nL})$, $T_{nL} = (E_{nL} - E_A)m_X/m_A$

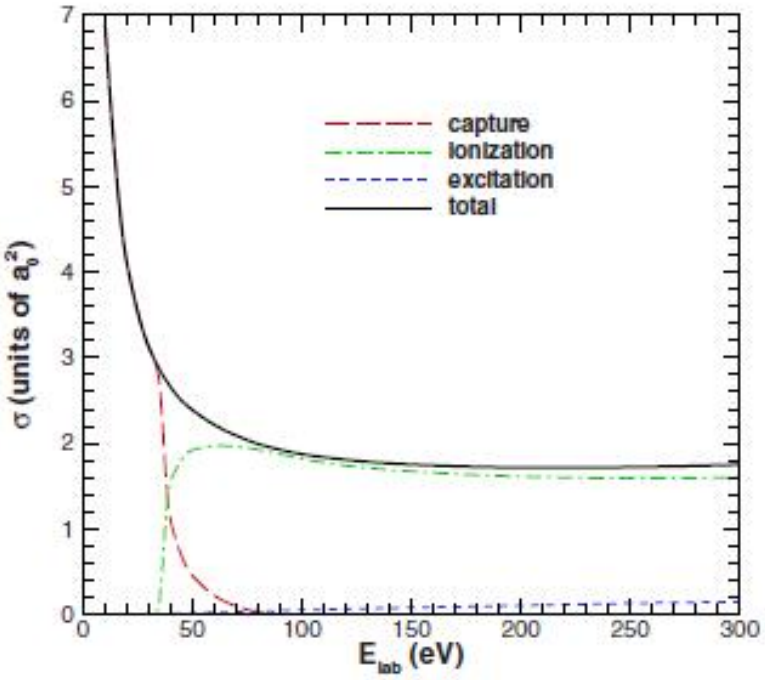


FIG. 7. (Color online) Capture (long-dashed curve), ionization (dot-dashed curve), excitation (short-dashed curve), and the total nonelastic (solid curve) cross sections for $\bar{p}$+He collisions. The integrated results of the differential cross sections shown in Fig. 6 are given by the sum of the ionization and excitation cross sections.

J.S.Cohen, Phys. Rev. A 78, 012509 (2008)

## More Sophisticated Theoretical Approaches

- Quasiclassical Diabatic-State Treatment
- Semiclassical approximation for coupled 2- and 3-body channels
- Fermion Molecular Dynamics method
- Full quantum consideration of $\bar{p} - A$ collisions at low velocities (ionization, excitation, atomic capture + kinetics) (?)

Review: J.S.Cohen, Rep. Prog. Phys. **67**, 1769 (2004)

Simple model "Black body with potential tale" gives correct general picture of antiprotonic helium formation. Advanced theory refines detailed primary populations and kinetic energy distribution.

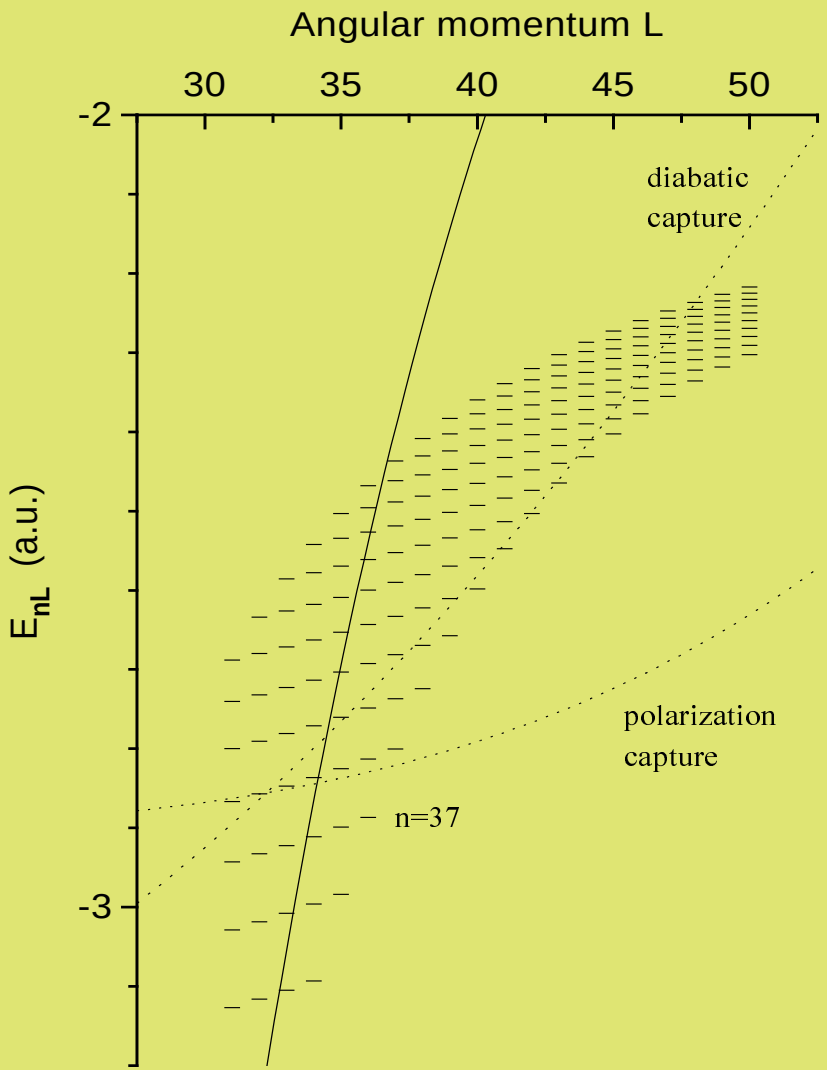


Metastability and population areas

Metastable states of $(\bar{p}He^+)^*$: circular & nearly-circular orbits with large $L$

For these states all transitions are strongly suppressed:
radiative transitions: $\lambda_\gamma \sim \mu Z_{eff}^2/(n^3L^2)\cdot 12$ ns$^{-1}$
Auger transitions: large $\Delta L_{Auger}$
collisional quenching is suppressed, at least, at thermal velocities, due to repulsion between $(\bar{p}He^+)^*$ and He

Metastability condition:
$\lambda_{Auger} < \lambda_\gamma \Rightarrow \Delta L_{Auger} \geq 4$

$$E_{nL} < -\frac{\mu Z^2}{2(L-2)^2}$$

$$L > 2 + \sqrt{2\mu/|E_{nL}|}$$

## 3. Elementary Processes of $(\bar{\mathbf{p}}\mathbf{He}^+)^*$ Collisions with He Atoms

Elastic scattering

$$(\bar{p}He^+)_{nL} + He \rightarrow (\bar{p}He^+)_{nL} + He$$

Sliding (''Stark'') transitions (without change of $n$)

$$(\bar{p}He^+)_{nL} + He \rightarrow (\bar{p}He^+)_{nL'} + He$$

Inelastic scattering with change of $n$ ($n' < n$ )

$$(\bar{p}He^+)_{nL} + He \rightarrow (\bar{p}He^+)_{n'L'} + He$$

Triple collisions and formation of dimers

$$(\bar{p}He^+)_{nL} + He + He \Rightarrow \begin{cases} (\bar{p}He^+)_{n'L'} + He + He \\ \left[(\bar{p}He^+)_{nL} He\right] + He \end{cases}$$

Transitions between HFS sublevels ($F = L \pm 1/2$, $J = F \pm 1/2$)

$$(\bar{p}He^+)_{nLFJ} + He \rightarrow (\bar{p}He^+)_{nLF'J'} + He$$

| Elementary process | Effects on kinetics |
|---|---|
| Elastic scattering | thermalization, competition between thermalization and *hot* quenching, shift and broadening of E1-spectral lines |
| Sliding transitions, $L \rightarrow L'$ | hot and thermal quenching |
| Inelastic scattering, $n \rightarrow n'$ | acceleration and quenching |
| Triple collisions | non-linear density dependence of quenching |
| HFS transitions, $F \rightarrow F'$ | relaxation of HFS sublevel populations, shift and broadening of M1-spectral lines |

# Elastic scattering of $(\bar{p}He^+)^*$ on He atoms

Model potential $V_0(R) = C_6(r_c^2 - R^2)/(R^2 + r_0^2)^4$ ($C_6 = 2.82$, $r_0 = 2.8$, $r_c = 3.0$ a.u.)

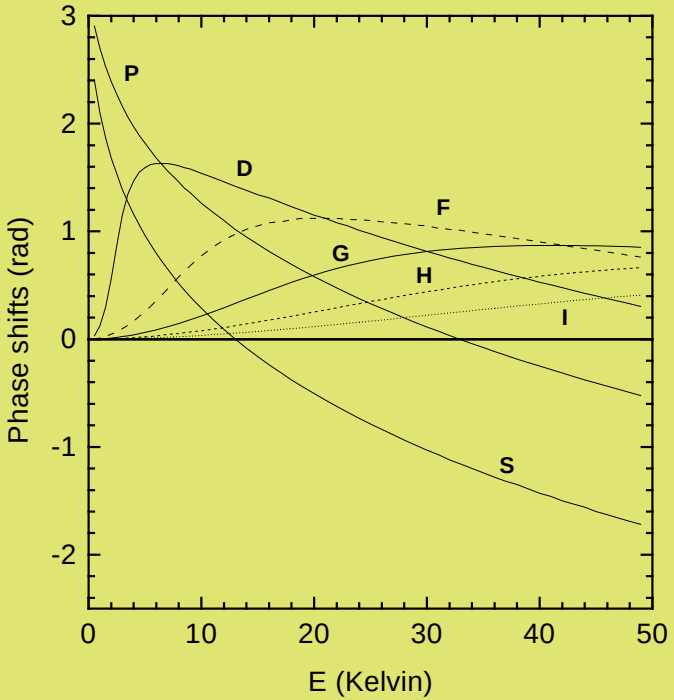


*P*hase shifts of $(\bar{p}He^+) - He$ scattering

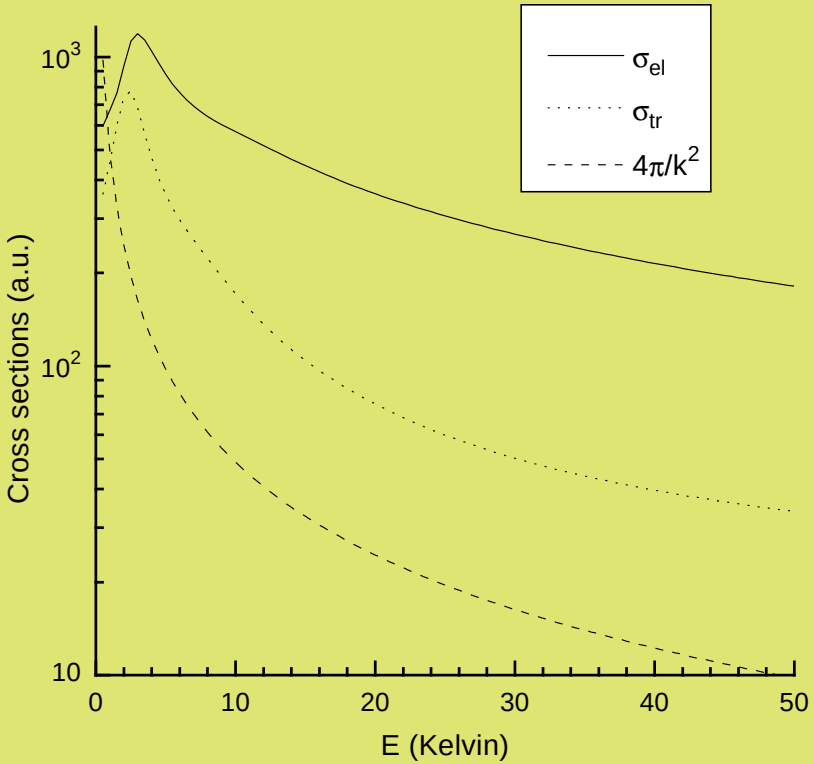


*E*lastic and transport cross sections

S, P, D-wave resonances at $E \sim (2-4)$ K; Possible $[(\bar{p}He^+)^*He]$ dimer bound states.

Note: $\sigma_{el} \gg \sigma_{tr}$ at $E > 20$ K; $\sigma_{el}$, $\sigma_{tr} \gg \sigma_{geom}$ at $E < 100$ K,

Per-atom stopping power due to elastic collisions:

$$\kappa(v) = (E_L/2)\,\xi\,\sigma_{tr}(v)$$

$\xi = 4M_1M_A/(M_1+M_A)^2 \simeq 0.988$. Continuous energy-loss: $\langle \Delta E_L \rangle = \kappa/\sigma_{el} \ll E_L$ ($\sigma_{tr} \ll 2\sigma_{el}$). Rate of energy loss:

$$dE/dt = -Nv\kappa(v)$$

Time of slowing-down from $v_i$ to $v_T$:

$$t(v_i \to v_T) = (M_1/N)\int_{v_T}^{v_i} dv/\kappa(v),$$

$$v_{nL}^2 = 2m_p(E_{nL} - E_0)/(M_AM_1),$$

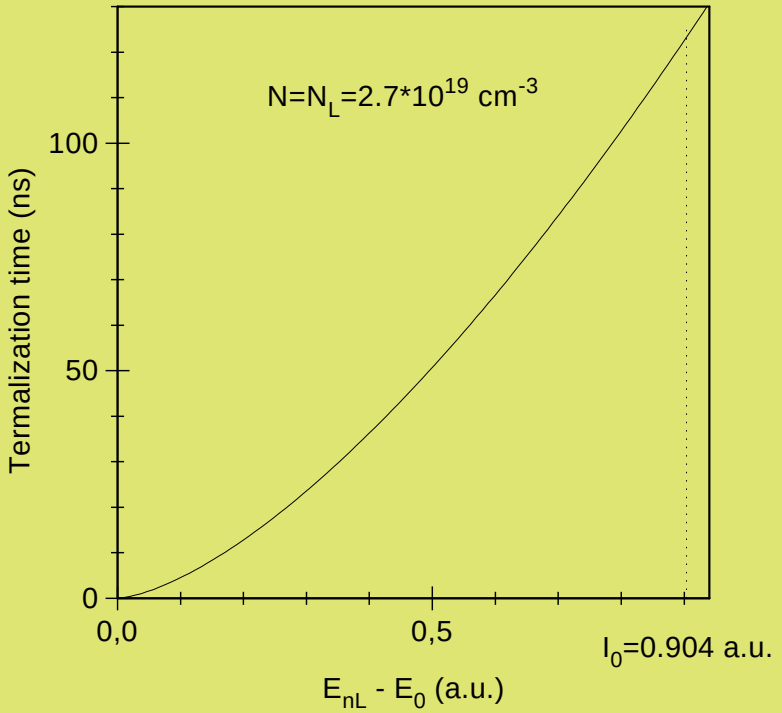


Thermalization time depending on initial level energy

## Collisional quenching of hot metastable $(\bar{p}He^+)^*$

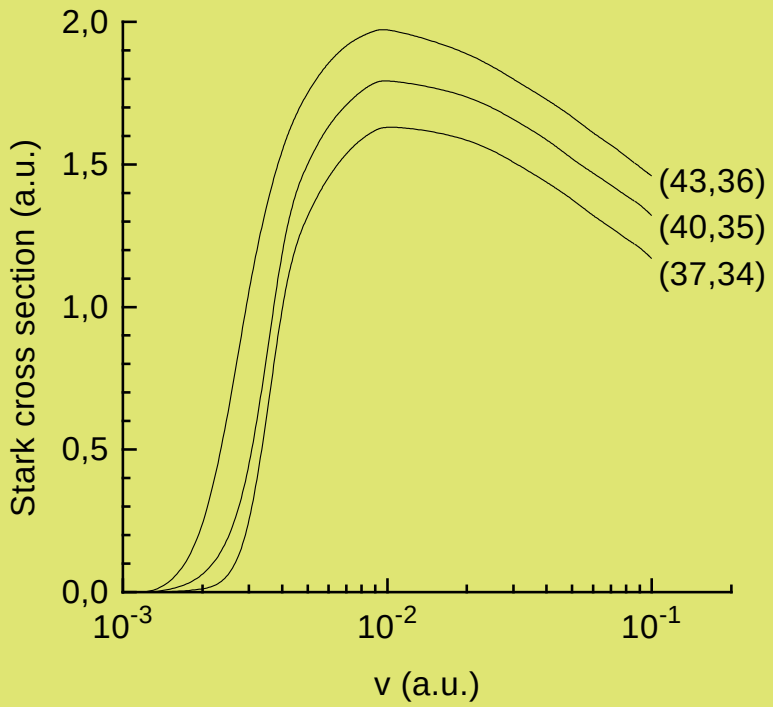


Stark transition ($\Delta L = \pm 1$) cross section *vs.* v

Effective "threshold" at $v = v_c \simeq (2 \div 3) \cdot 10^{-3}$ corresponds to the value of Massey parameter $\eta = \Delta E \cdot R/(\hbar v) \sim 1$

Survival probability during slowing-down from $v_i$ to $v$:

$$P(v_i \to v) = \exp\left[-\int_v^{v_i} \sigma_q(v) M_1 v \, dv / \kappa(v)\right]$$

Note: $P(v_i \to v)$ independent on density.

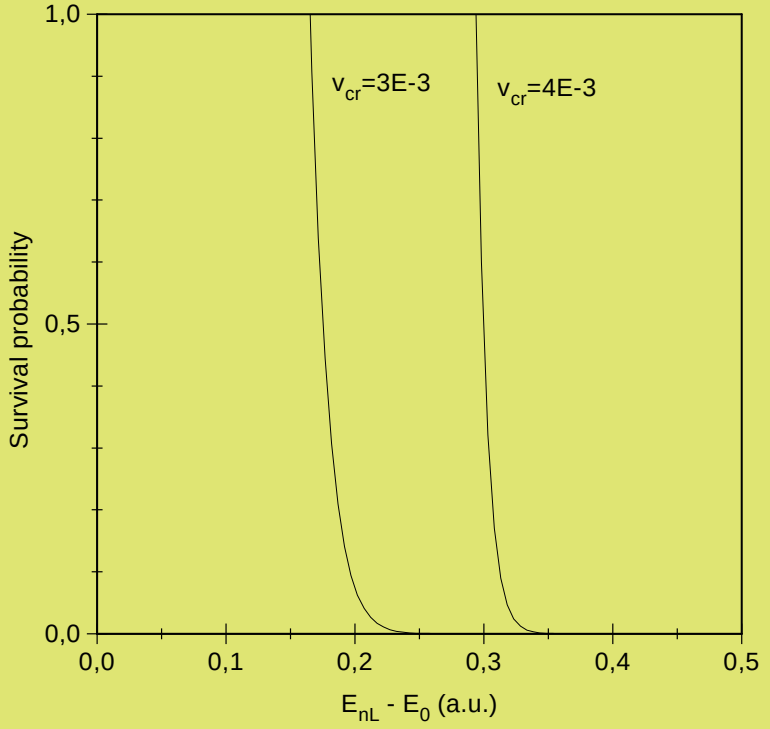


Probability of survival to $v = v_{cr}$ depending on initial level energy

## Survival probability depending on time

Slowing-down time $t(v_i \to v) \Longrightarrow$ inverse function $v = v(t; v_i)$, and

$$P(t; v_i) = P(v_i \to v(t; v_i))$$

depend on density due to $v(t)$ (scaling variable $\tau = t\phi$, $\phi = N/N_L$)

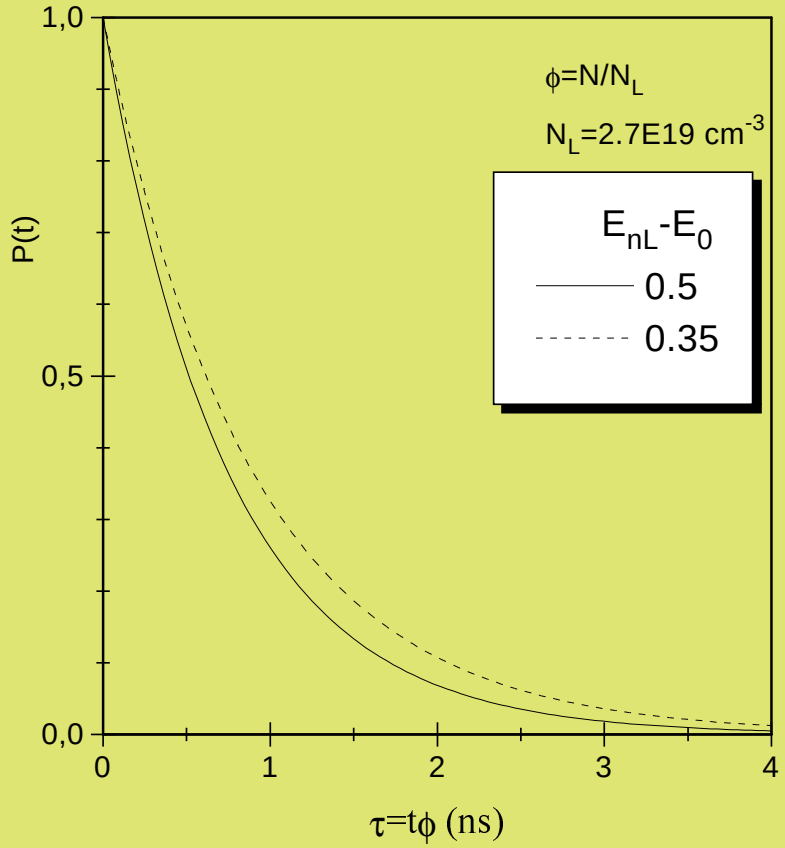


Time dependence of survival probability

## Collisional quenching of thermalized $(\bar{p}He^+)^*$ and lifetimes

Collisional transitions of thermalized $(\bar{p}He^+)^*$ are strongly suppressed as compare with hot atoms due to large Massey parameter $\eta \gg 1$.

Experimental data (M. Hori et al.): Lifetimes of $(\bar{p}He^+)^*$ as a function of the helium target density: for the state (39, 35) a lifetime practically independent on density ($\tau \simeq 1.5\,\mu s$) up to liquid helium, whereas for the state (37, 34) $\tau$ decreases from $1.2\,\mu s$ to $130\,ns$ with increasing density from $1 \cdot 10^{20}$ to $6 \cdot 10^{21}$ cm$^{-3}$.

Why collisional quenching effects for these states are so qualitatively different?

Existing theoretical calculations unable to explain this puzzle

TABLE II. Slope $s=\partial\lambda/\partial N$ of the collisional quenching rate, in cm$^3$ s$^{-1}$.

| $(n,l)$ | Experiment [4] | Perturbation theory | Coupled-channel calc |
|---|---|---|---|
| (39,35) | $(2.5\pm1.9)\times10^{-18}$ | $1.5\times10^{-18}$ | $1.6\times10^{-18}$ |
| (37,34) | $(1.2\pm0.2)\times10^{-15}$ | $3.1\times10^{-19}$ | $3.2\times10^{-19}$ |

B.D. Obreshkov, D.D. Bakalov, B. Lepetit, K. Szalewicz, Phys. Rev. A 69 (2004) 042701

Collisional quenching of $(\bar{p}He^+)^*$ by admixtures:
a wide variety of questions to theory

## Shift and broadening of E1 spectral lines

General theory of shift and broadening of spectral lines is well know
(Peach G 1996 Collisional broadening of spectral lines Atomic, in: Molecular and Optical Physics Handbook, ed. G.W.F. Drake, New York: AIP, chapter 57)

The problems are: effective interaction for specific system $\Rightarrow$ S-matrix $\Rightarrow$ $\Delta(v) - \mathrm{i}\gamma(v)$, then average over thermal motion

Main qualitative features of the experimental data for $\Delta$ and $\gamma$ can be explained using the model interaction potential $V_0(R)$ (G.Korenman 1999)

More sophisticated approach (quantum-chemistry potential energy surface) allow to obtain a qualitative agreement with the experimental data (D.Bakalov et al., Phys. Rev. Letters 84 (2000) 2350)

## 4. Effects of collisions on HFS states

Problems:

a. Collisional transitions between HFS states
b. Shift and broadening of M1 spectral lines
c. Kinetics of HFS transitions in presence of resonance MW field

Model of Interaction between $(\bar{\mathbf{p}}\mathbf{He}^+)^*$ and He atom

$$\langle nL\Lambda|V(\mathbf{R},\xi)|nL\Lambda'\rangle = V_0(R)\delta_{\Lambda\Lambda'} + V_2(R)\sum_\nu \langle L\Lambda' 2\nu|L\Lambda\rangle Y^*_{2\nu}(\mathbf{n})\sqrt{4\pi/5},$$

where $\xi$ is a set of inner coordinates, $\mathbf{R}$ is a vector of relative coordinates between two sub-systems, and $\mathbf{n} = \mathbf{R}/R$.

Radial dependencies of scalar and tensor interactions are similar, except for a very small distance,

$$\begin{aligned} V_0(R) &= C_6 f(R) \\ V_2(R) &= G_6 f(R)[1 - \exp(-\eta R^2)] \\ f(R) &= (r_c^2 - R^2)/(R^2 + r_0^2)^4 \end{aligned}$$

Parameter $\eta$ is a large enough ($\sim 10$ a.u.) to avoid its influence at $R > 1$ a.u.

(See poster by S.Yudin for further details)

## Results for collisional HFS effects

1. Rates of collisional HFS transitions in antiprotonic $^3$He and 4He are comparable by order of value for the similar types of transition:
single spin-flip transitions $\sim 10^6\, s^{-1}$,
double spin-flip transitions $\sim 10^3\, s^{-1}$,
triple spin-flip transitions $\sim 10^0\, s^{-1}$, at T=6 K, N=$3 \cdot 10^{20}\, cm^{-3}$.
Isotope effect for the similar transitions gives a factor of about 1.5- 2.

2. Collisional shifts of the M1 spectral lines are very small: $1 \cdot 10^4\, s^{-1}$ (1.6 kHz) for 4He, $2.5 \cdot 10^4\, s^{-1}$ (4 kHz) for 3He at the same T and N, i.e., much less than the achieved experimental accuracy.

3. Collisional broadening of the M1 spectral lines at T=6 K, N=$3 \cdot 10^{20}\, cm^{-3}$ is about 0.3 MHz for $^4$He, 0.4 MHz for $^3$He. These values consist 12-18 % of the total line widths. Total widths of the spectral lines are calculated by solving a master equation for the density matrix of the system in the MW radiation with account for the Fourier width and collisional broadening. The obtained total widths are compatible with the observed values.

4. Collisional transition rates, shifts and broadenings of M1 spectral lines decrease by several times with increasing temperature from 2 K to 10 K due to the resonance scattering of antiprotonic helium on He atom at energy about 3-4 K for $^4$He and 1 K for $^3$He.

5. Dependence of the ratio $p_{on}/p_{off}$ on $t_d$ for $^4$He, as well as this value at $t_d = 350\, ns$ for $^3$He are in agreement with the corresponding experimental results.

## 5. Effective annihilation rates of antiprotonic helium ions ($\bar{p}He^{2+}$)*

### Experimental data

M. Hori et al., PRL 94 (2005) 063401

Effective annihilation rates of $(\bar{p}He^{2+})_{nl}$ for long-lived states $l = n-1, n = 28 \div 32$ were measured *vs.* density ($3 \cdot 10^{16} - 2 \cdot 10^{18}\, cm^{-3}$) at T=10 K for two He isotopes.

Estimated quenching cross section $\sigma \sim (4 - 10) \cdot 10^{-15}\, cm^2 = (140 - 360) a_0^2$ is huge

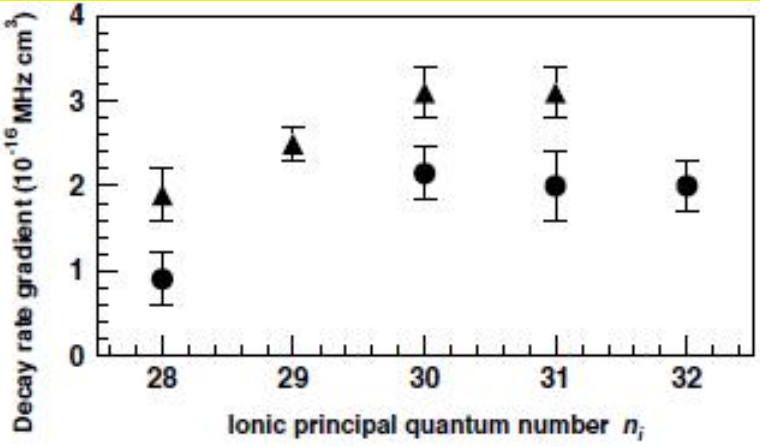


FIG. 4. Gradients of the decay rates per target density of four $\overline{p}\,^4He^{2+}$ (indicated by filled circles) and $\overline{p}\,^3He^{2+}$ (triangles) ionic states, as a function of the principal quantum number $n_i$.

Earlier calculations (at $T \sim 10^4$ K) give Stark cross section less by order of value. What are the quenching mechanisms?

We have considered Stark transition using coupled channels approach with *ab initio* PES potential

Energy dependence of the Stark cross section for the circular orbit with $n = 30$

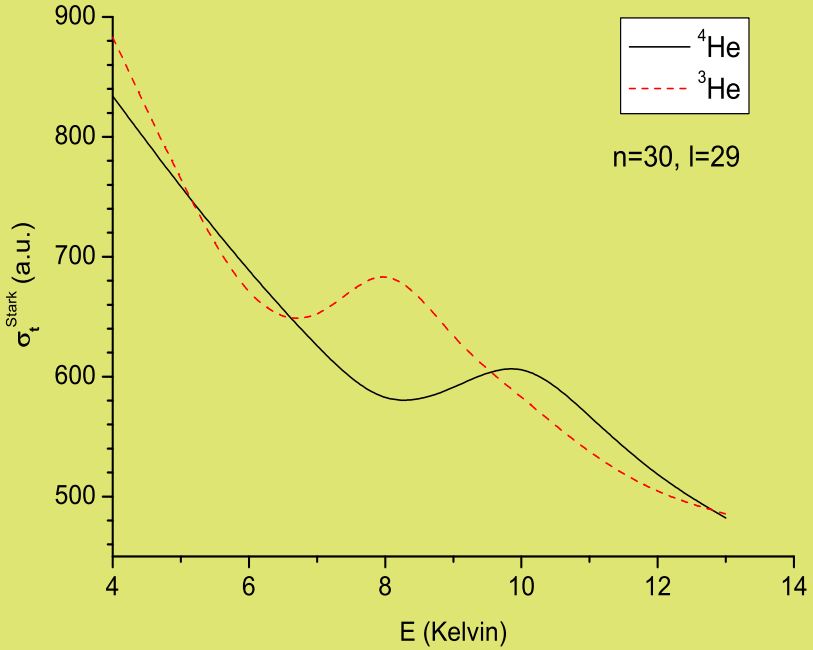


Dependence of the Stark cross section on principal quantum number $n$ and isotope, for the circular orbit

| | $n$ | | | | |
|---|---|---|---|---|---|
| isotope | 28 | 29 | 30 | 31 | 32 |
| $^4$He | 574 | 598 | 620 | 636 | 649 |
| $^3$He | 539 | 566 | 583 | 597 | 605 |

Per-atom rates of Stark transitions from circular orbits, averaged over thermal motion, $\kappa = \langle v\sigma \rangle$ (units: $10^{-15}\,\mathrm{MHz}\cdot\mathrm{cm}^3$)

| isotope | $n$ | | |
|---|---|---|---|
| | 28 | 30 | 32 |
| $^4$He | 3.77 | 4.15 | 4.46 |
| $^3$He | 4.46 | 4.82 | 5.01 |

Experiment: $d\gamma/d\rho \sim (1 \div 3)\cdot 10^{-16}\,\mathrm{MHz}\cdot\mathrm{cm}^3$

(units conversion: a.u.$=v_a a_0^3 = 6.126\times 10^{-9}\,\mathrm{cm}^3/\mathrm{s} = 6.126\times 10^{-15}\,\mathrm{MHz}\cdot\mathrm{cm}^3$)

Collisional Stark transitions give a most important contribution to effective annihilation rates. The calculated Stark and induced annihilation cross sections, as well as effective cascade rates $\lambda_{eff}$ allow to understand the measured values of $\gamma_n$ by order of value. But they are insufficient for the quantitative explanation.

In conclusion, an experimental study of long-lived antiprotonic helium during 20 years has given extensive material for the theory of collisions between antiprotonic helium and atoms. Further theoretical efforts are needed for a more detailed understanding of the phenomena.

THANK YOU!